Mechanistic insights into sulfur rich oil formation, relevant to geological carbon storage routes. A study using (+) APPI FTICR-MS analysis

Renzo C. Silva*, Calista Yim, Jagoš R. Radović, Melisa Brown, Priyanthi Weerawardhena, Haiping Huang, Lloyd R. Snowdon, Thomas B.P. Oldenburg, Steve R. Larter

PRG, Department of Geoscience, University of Calgary, 2500 University Drive NW, T2N 1N4, Calgary, AB, Canada.

*rcsilva@ucalgary.ca

THIS MANUSCRIPT VERSION HAS BEEN ACCEPTED FOR PUBLICATION IN

ORGANIC GEOCHEMISTRY

https://doi.org/10.1016/j.orggeochem.2020.104067

Mechanistic insights into sulfur rich oil formation, relevant to geological carbon storage routes. A study using (+) APPI FTICR-MS analysis

Renzo C. Silva*, Calista Yim, Jagoš R. Radović, Melisa Brown, Priyanthi Weerawardhena, Haiping Huang, Lloyd R. Snowdon, Thomas B.P. Oldenburg, Steve R. Larter

PRG, Department of Geoscience, University of Calgary, 2500 University Drive NW, T2N 1N4, Calgary, AB, Canada.

KEYWORDS: organosulfur compounds; organic geochemistry; FTICR-MS; crude oil; carbon sequestration

Abstract

Sulfur incorporation into sedimentary organic matter has a key role in carbon preservation in the geosphere. Such processes can inform strategies for human timescale carbon storage to mitigate climate change impacts and thus more detailed knowledge of sulfur incorporation into biomass species is needed. Until recently, detailed chemical characterization of sulfurized organic matter was only possible by analyzing individual building blocks obtained after desulfurization reactions. In this study, Fourier transform ion cyclotron resonance mass spectrometry (FTICR-MS), with atmospheric pressure photoionization in positive ion mode, (+) APPI, was used to investigate the chemical composition of sulfur rich crude oils and to obtain mechanistic insights into the sulfur incorporation reactions happening during early diagenesis. Contrary to expectations, (+) APPI FTICR-MS data show that sulfurized lipids (with up to 6 sulfur atoms and up to *m/z* 1100) occur as free molecules in these oils, rather than within a macromolecular network linked by (poly)sulfide bridges. In contrast to the mature Peace River (Canada) oils, the thermally immature Rozel Point (USA) and Jianghan Basin (China) oils show a carbon number preference in sulfurized species resembling biogenic precursor molecules, which highlights the importance of S-bound molecules as geochemical proxies for early diagenetic processes. This study indicates that sulfur incorporation reactions involve the formation of S-cyclic structures in which the double bond equivalent is $\geq$ the number of S atoms. Collision induced dissociation

(CID-) FTICR-MS experiments suggest the occurrence of intermolecular sulfur incorporation reactions, but only as a mechanism that is secondary to intramolecular sulfur addition. The CID-FTICR-MS experiments indicated that steroid sulfurization typically yields S-bearing cyclic structures and that thiol/thioether groups may be present throughout the chemical matrix but only to a minor extent. In addition, CID-FTICR-MS also confirms the occurrence of sulfurized alkenones in low maturity oils. Knowledge of organic sulfur molecule formation informs routes for carbon dioxide removal technologies that could be used to sequester carbon in the geosphere and/or hydrosphere in the form of recalcitrant organic species.

1. Introduction

Sulfur incorporation into sedimentary organic matter has a key role in carbon preservation in the geosphere, not only on Earth but also possibly on Mars (Werne et al., 2004; Summons et al., 2011). The understanding of mechanisms and geochemical implications of sulfur incorporation reactions expanded greatly during the late 1980s and early 1990s (Orr and Sinninghe Damsté, 1990; Aizenshtat et al., 1995; Amrani, 2014), and given their relevant role in enabling an important carbon sink, there are still many active areas of research in the field. For example, there currently exists a heightened research interest to further understand carbon preservation mechanisms via sulfur incorporation (Raven et al., 2016; Pohlabeln et al., 2017) in the context of the global change and the need to keep the global temperature increase to <2 °C by the end of this century (IPCC, 2018).

Large scales of carbon removal are not unusual in natural systems. The global ocean has pools of organic carbon found in dissolved and particulate form in the water column, or deposited in the deep-sea sediments that are of similar magnitude to atmospheric carbon reservoirs (Houghton, 2007; Hansell et al., 2009; Jiao et al., 2010). Therefore, a better understanding of natural mechanisms for long term preservation of organic molecules in the geosphere can provide guidelines for the development of technologies that artificially enhance the removal of carbon from the atmosphere to ocean or subsurface reservoirs, in the form of biologically refractory organic species analogous to those already present naturally in the Earth. Kinetics and feedback mechanisms of any engineered interventions within natural organic matter pools will be crucial variables to achieve net negative carbon drawdown from the atmosphere on the timescales relevant for anthropogenic climate intervention (hundreds to thousands of years).

During the early diagenesis, sulfurized organic compounds, commonly occurring in anoxic environments that are rich in reduced sulfur, typically resemble their biological precursors. As the diagenesis progresses, extensive sulfurization reactions enable multi-point, intermolecular cross-linkage, eventually generating the macromolecular structures that are the building blocks of sulfur rich kerogen (type II-S) (Tegelaar et al., 1989; Vandenbroucke and Largeau, 2007). Sulfur rich macromolecular structures were also detected in thermally immature, sulfur rich oils (Sinninghe Damsté et al., 1987; Sinninghe Damsté et al., 1989; Orr and Sinninghe Damsté,

1990). However, the detailed chemical characterization of such compounds was only possible by analyzing individual building blocks after desulfurization reactions (Adam et al., 1992; Adam et al., 1993; Richnow et al., 1993). Since then, analytical technologies have greatly advanced. Ultrahigh resolution mass spectrometry, in particular the FTICR-MS (Fourier transform ion cyclotron resonance mass spectrometry) technology, has enabled the identification of several thousand peaks in complex organic mixtures, revolutionizing the understanding of the petroleome (Marshall and Rodgers, 2008). In the field of organic geochemistry, such technical advances were translated into an unprecedented capability to probe the high molecular weight, polar compounds at a high level of detail, expanding the way biodegradation, thermal stress and other biogeochemical processes are understood (Oldenburg et al., 2014; Radović et al., 2015; Radović et al., 2016b; Oldenburg et al., 2017).

Investigations focused on the geochemical significance of sulfur species have also greatly benefited from ultrahigh resolution mass spectrometry applications. Hughey et al. (2004) analyzed two same sourced Smackover Formation oils of different levels of thermal maturity using (-) ESI (electrospray ionization in negative ion mode) FTICR-MS, suggesting the removal of sulfur and oxygen compounds was promoted by thermal maturation. Similarly, Oldenburg et al. (2014) reported that the relative apparent abundances of all heteroatom-containing compound classes (nitrogen, oxygen, sulfur and mixed heteroatom species) detected in that study decreased systematically with increasing oil maturation levels. Walters et al. (2015) used both (+) APPI (atmospheric pressure photoionization in positive-ion mode) and (-) ESI FTICR-MS to probe sulfur compounds and oxygenated analogs present in samples from the Smackover Formation, revealing intermediates (classes O_x and SO_x) of thermochemical sulfate reduction (TSR) redox reactions. A similar approach detected the formation of TSR induced proto-solid bitumen, including highly condensed polynuclear aromatic and naphthenoaromatic species with up to three sulfur atoms (Walters et al., 2011). Lu et al. (2013) used (+) ESI (electrospray ionization in positive-ion mode) FTICR-MS to investigate sulfur rich heavy oils from Bohai Bay Basin, reporting a wide range of sulfurized sedimentary steroids in addition to a complex distribution of sulfur and oxidized sulfur compounds. Based on a similar approach, Lu et al. (2014) detected high levels of alkylcyclothioethers within Jianghan Basin oils. More recently, Liu et al. (2018) reported an in-depth investigation of polar sulfur compounds in immature crude oils from the

Jianghan Basin via (-) ESI and (+) ESI FTICR-MS showing that the detected S-bearing species are mostly cyclic, originating from intramolecular sulfurization of functionalized precursors during early diagenesis. The authors inferred that the extent of intramolecular sulfurization is based on the number of reactive functional groups in the precursor molecule.

Expanding on these findings, the present study investigates the compounds present in a suite of sulfur rich oils and their fractions via (+) APPI FTICR-MS and (+) APPI CID-FTICR-MS experiments. (+) APPI is the ionization technique of choice for sulfur-rich sample analysis due to its enhanced ability to ionize sulfur compounds in complex organic mixtures without chemical derivatization or special sample preparation strategies (Purcell et al., 2006; Oldenburg et al., 2014). Extended compositional information of high molecular weight, sulfur bearing molecules that could not be detected in earlier GC based studies are presented and critically discussed based on the current understanding of sulfur incorporation into organic matter. This paper aims to gather new insights from sulfur rich oil molecular composition to probe the mechanisms of sulfur incorporation into sedimentary organic matter, which could possibly be leveraged for the development of carbon dioxide removal (CDR) technologies.

2. Materials and methods

2.1. Sample set description

Five sulfur rich oils from different basins were selected in this study: (a) three high maturity, highly biodegraded oils from the Peace River area, Canada; (b) one immature oil from the Jianghan Basin, Eastern China; and (c) one immature oil from the Rozel Point, Utah, USA (Table 1).

Rozel Point is an immature, sulfur-rich heavy oil generated from a hypersaline, lacustrine source rock of Miocene age (Meissner et al., 1984; ten Haven et al., 1988; Sinninghe Damsté et al., 1989). High concentrations of organic sulfur (up to 15 wt%) and the unique depositional environment that characterizes Rozel Point oil have motivated many studies of the origin and fate of organically bonded sulfur during early diagenesis, with implications for the understanding of Type II-S kerogen formation (Eglinton et al., 1994). The Jianghan Basin, located in eastern China, is comprised of five major tectonic units with most oil production occurring in the Qianjiang depression from the Eocene Qianjiang Formation (Philp and Zhaoan, 1987). Oils from

the Qianjiang depression are generated from the Qianjiang Formation and Xingouzui Formation, which were deposited in anoxic, sulfate reducing and saline lacustrine environments during the early Cretaceous to Paleogene (Carroll and Bohacs, 2001; Hou et al., 2017). Due to cycles of marine transgression and progradation activity, hot paleoclimate, and clastic sediment deposition from lacustrine systems, over 220 evaporitic layers interlaced with shales and sandstones formed the Jianghan Basin source rocks (Philp and Zhaoan, 1987; Peirong et al., 2008; Hou et al., 2017). The Qianjiang Formation acts as both source and reservoir (Philp and Zhaoan, 1987; Huang and Hinnov, 2014; Hou et al., 2017). Upper Qianjiang sections act as the oil reservoir while the deeper sections and Xingouzui Formation embody the source rock. Oils from the Qianjiang Formation typically exhibit a pronounced even/odd *n*-alkane predominance, low ratios of Pr/Ph and high ratios of gammacerane/hopane, indicating a highly anoxic, reducing and saline depositional environment (Philp and Zhaoan, 1987). The Peace River oil sands, located in northwestern Alberta, is one of three major bitumen deposits in that province. The Peace River area is comprised of two main groups, the Bullhead Group formed by the Cadomin and Gething formations, and the overlying Fort St. John Group which, in succession, comprises the Bluesky, Spirit River, Peace River and Shaftesbury formations. Peace River oil reservoirs, Bluesky, Gething and McMurray, are late Paleozoic to Mesozoic in age and are charged by Cretaceous oil source rocks (Adams et al., 2012). The reservoirs are supplied with a mixture of hydrocarbons expelled from multiple source rocks including the Nordegg Member of the Fernie Formation, Gordondale Formation and Permian Doig Formation (Riediger, 1994; Adams et al., 2013). Manville Group Bluesky and Gething reservoirs may also be vertically charged by the Mississippian Exshaw-Banff formations where hydrocarbons migrated upwards into permeable Cretaceous sand units when erosion deteriorated the Poker Chip shale seal (Allan and Creaney, 1991). Peace River bitumen, which exhibits high levels of biodegradation, such as those from the Bluesky Formation, are sourced by Exshaw-Banff source rock as these oils had a longer residence time in the reservoir. On the other hand, deposits in the western part of Peace River received more significant contributions from Gordondale source rock as these oils are higher in sulfur content, less mature and have greater API gravity (Adams et al., 2013).

2.2. Non-polar macromolecular fractions

The experimental procedure used to obtain the non-polar macromolecular fraction (NPMF) from Rozel Point and Jianghan oils was adapted from Adam et al. (1993). In brief, aliquots of the crude oils (~100 mg) were loaded on a silica gel (6.0 g, 220-440 mesh) column. The samples were washed with 50 mL of hexane and then eluted with 15 mL of hexane:diethyl ether (98:2), which yielded the NPMF orange-colored band that was collected, evaporated to dryness and submitted to (+) APPI FTICR-MS analysis. NPFM was not produced from western Canadian oils indicating that the macromolecular fraction was not present in such mature and overmature oils.

2.3.Mass spectrometry

Two primary ionization mechanisms are expected to occur in the APPI source: proton transfer, which generates even electron protonated ions depending on the proton affinity of the analyte; and the formation of an odd electron radical ion species (Raffaelli and Saba, 2003). Note that the thermospray conditions in (+) APPI show negligible in-source thermal alteration of species (Bagag et al., 2008).

Even though it was demonstrated in previous studies that (+) APPI FTICR-MS has some very rudimentary quantitation capabilities (Oldenburg et al., 2014), due to unassessed differences in ionization responses, intensities cannot be assumed to reflect the actual abundance of compounds present in the sample. Thus, quantitative aspects of compounds and heteroatom classes are not considered herein; only relative intensities are discussed, based on monoisotopic peak intensities of assigned peaks (RMI, relative monoisotopic intensity). Also, structural discussions of detected species are only speculative, since FTICR-MS data provide unambiguous molecular formulas but cannot distinguish isomers.

Attempts to perform CID-FTICR-MS experiments in complex mixtures provide limited but potentially useful information about the chemical structure of detected ions. Targeted peaks may represent a dozen to potentially thousands of different isomers, as no prior chromatographic clean-up was performed in these experiments. Therefore, the measured fragmentation patterns represent the conflation of the fragmentation patterns of all the isomers with the targeted molecular formula. The isolation window of the parent peak ($m/z \pm 0.4$) used in this study may contain 10+ peaks. Thus, only peaks with the highest intensity within their $m/z \pm 0.4$ spectral

windows were selected for CID-FTICR-MS experiments to minimize interferences with non-target peaks. This strategy limits the number of available targets, which have to be both geochemically relevant and the dominant peak in its *m/z* ± 0.4 spectral window. To further reduce interferences with fragments originating from other parent peaks within the *m/z* ± 0.4 windows, peaks with more carbon or sulfur atoms than the parent ion were ignored. Peaks detected in CID-FTICR-MS experiments were assigned molecular formulae with assignment errors < 100 ppb.

2.3.1. (+) APPI *FTICR-MS method*

The samples were analyzed using a 12 T Bruker SolariX FTICR-MS instrument. Whole oil and fractions were diluted to 0.25 mg/mL in toluene and then infused into the ionization source using a syringe pump set to deliver 200 µL/h. Atmospheric pressure photoionization in positive ion mode via a krypton lamp at 10.6 eV was used to ionize the samples. Transfer capillary temperature and nebulizer pressure were set to 350 °C and 1.0 bar, respectively. Reserpine ($C_{33}H_{40}N_2O_9$) was added to the sample solution to assess internal calibration efficiency. The instrument was tuned using a reference Athabasca whole bitumen sample. Ions ranging from *m/z* 150 to 1500 were isolated using a linear quadrupole and accumulated over 5 ms in the collision cell before being transferred to the ICR cell. Spectra were collected in absorption mode, using an algorithm proposed by Kilgour et al. (2013). Two hundred transients of 8 million points in the time domain were collected and summed to improve the experimental signal/noise ratio (S/N). FTICR–MS raw data were processed using the CaPA v.1.0 (Aphorist Inc.) software package. Peaks with S/N higher than 4 were assigned based on highly accurate *m/z* measurements and on stable isotopic distributions. Compositional boundaries, in terms of stoichiometry (element atom content) for the fitting algorithm, were set to $C_{4\text{-}95}H_{0\text{-}200}N_{0\text{-}2}S_{0\text{-}8}O_{0\text{-}5}$ and double bond equivalent (DBE) range, which is a measure of hydrogen deficiency due to double bonds and/or cyclic structures, was limited to be between 0 and 60. The mass spectra were recalibrated using homologous series present in the samples. Ragnarök v.2.0 (Aphorist Inc.) was used for data manipulation and visualization. The resulting list of molecular formulae and intensities is typically analyzed by summarizing the data based on three non-hierarchical layers: heteroatom class, DBE and carbon number. Heteroatom class describes the amount of the heteroatoms contained in a given molecular formula. The symbol “HC” is used for the class in which when no

heteroatom is present in the molecular formula, and classes detected as radical ions are differentiated from protonated ones by a dot following the class symbol.

2.3.2. (+) APPI CID-FTICR-MS method

A set of peaks found in the oils was selected for CID experiments (Sections 4.3, 4.4 and 4.7). Sulfur-bearing parent ions were isolated (*m/z* ± 0.4) in the linear quadrupole and accumulated over 0.3–1.0 s in the collision cell. The collision cell voltage was set to 12–20 V (compared to the regular operating level of 5 V) to achieve collision-induced dissociation (CID) conditions, causing the ions to undergo several low energy collisions with room temperature argon atoms. Ions in the collision cell (parent and daughters) were then transferred to the ICR cell and the CID-FTICR-MS spectra were collected in absorption mode after summing two hundred transients of 4 million points in the time domain. The instrument was tuned to detect ions ranging from *m/z* 150 to 1500, i.e. small molecular fragments (<*m/z* 150) fell outside the analytical window in these experiments. Bruker DataAnalysis v.4.4 and R v.3.4.0 software packages were used for data processing and visualization.

3. Results

3.1. Non-polar macromolecular fraction

The NPMF fractions represented 18 and 22 wt% of the Jianghan and Rozel Point oils, respectively, and their (+) APPI mass spectra are shown in Figure 1.

3.2. (+) APPI FTICR-MS of oils and their fractions

In all spectra acquired in this study, the isotopic pattern of ^{13}C peaks indicated the presence of singly charged species only. Averaged mass resolution ($m/\Delta m_{50\%}$) achieved for peaks detected between *m/z* 397 and 403 was higher than 1,015,000 and higher than 560,000 for peaks between *m/z* 797 and 803. Unique molecular formulas with absolute assignment error lower than 750 ppb were assigned to 40,967 monoisotopic peaks present in the oil samples spectra (Fig. 1). In each sample, peaks left unassigned represented less than 3% of total peak intensity and are not discussed further. Heteroatom classes with fewer than 25 peaks were also excluded from the discussion.

Fig. 2 shows the heteroatom class distribution of the investigated oils, as obtained by (+) APPI FTICR-MS, where radical ion classes are differentiated from protonated ones by a dot following the class symbol. The relative sulfur number distribution for the studied oils, as measured in classes $S\bullet_{1\text{-}6}$, is shown in Fig. 3A. Figs. 3B and 3C show the carbon number and DBE distribution of all detected molecular formulae within the oil set. Fig. 4 highlights the DBE distribution within the sulfur containing heteroatom classes, whereas Fig. 5 shows the carbon number distribution of heteroatomic classes $S\bullet_1$ DBE 5 and 6 species. Fig. 6 shows the carbon number distribution of heteroatomic classes S_1 DBE 1 and $S\bullet_1$ DBE 3. Fig. 7 shows the DBE distribution of C_{40} species within class $S\bullet_{1\text{-}5}$ as found in Rozel Point and Jianghan oils, whereas Fig. 8 shows the heteroatomic class $S\bullet_1$ DBE 8 carbon distribution for the same oils.

3.3. (+) APPI CID-FTICR-MS

CID experiments were set to investigate the fragmentation patterns of a few selected parent ions by measuring fragments with $m/z > 150$. Tables 2 and 3 show results of the CID-FTCIR-MS experiments used to investigate S_1 DBE 5 $C_{27\text{-}30}$ and $S_2\bullet$ DBE 11 $C_{56\text{-}57}$ species, respectively. The target ion selection was based in the experiments described in Section 3.2 and will be further discussed throughout Sections 4.3 – 4.7.

4. Discussion

Whereas the GC-MS, on which most of previous work is based, is limited to targeting specific amenable compound isomers that may be present in very small concentrations, FTICR-MS data represents conflation of individual compounds into compound classes, DBE and carbon numbers, and are more representative of bulk properties. A direct comparison between previous work that used a combination of desulfurization reactions and GC-MS analysis, and the current study using FTICR-MS data is not possible given the different analytical capabilities of these technologies, each with different limitations and advantages. Throughout this discussion section, we refer to and use literature results based on GC-MS analysis to support interpretations based on the FTICR-MS data. The ability to study molecules without the need of chemically modifying the matrix via desulfurization reactions brings new observations worthy of discussion given their impacts on the understanding of sulfurization reactions occurring in the geosphere.

4.1. NPMF and sulfur-bridged (macro)molecules

The current understanding of organic matter sulfurization mechanisms assumes the substitution of functional groups in the precursor molecules by sulfur atoms, which then can rearrange to more stable forms such as thiolanes and thiophenes, and/or act as bridges linking two precursor molecules. As diagenesis progresses, such linkages would propagate and eventually generate a Type II-S kerogen, which can produce oil molecules at a much lower level of thermal stress than other kerogen types (Tegelaar et al., 1989; Vandenbroucke and Largeau, 2007).

Adam et al. (1993) reported a hexane soluble nonpolar macromolecular fraction (NPMF) occurring in sulfur rich oils (including the RP oil), composed of highly aliphatic, high molecular weight structures, possibly cross-linked by sulfur in a process similar to natural vulcanization. Through a stepwise selective sulfur removal procedure, Richnow et al. (1993) proposed that in RP oil, *n*-alkanes, hopanoids, steroids and phytanes are bound simultaneously via oxygen, sulfur and aromatic units, based on the position of the functionality in the precursor molecules, creating a macromolecular matrix. Alcohols released in the desulfurization of RP oil NPMF can be as abundant as hydrocarbons and exhibited a similar carbon number distribution to hydrocarbons, but the origin of most species could not be assigned (Jenisch-Anton et al., 1999). Efforts to chemically or physically degrade such macromolecular organic matter were needed to circumvent the inability of gas chromatography to analyze sulfur-rich macromolecules (Jenisch-Anton et al., 1999). Investigating the RP oil, Adam et al. (1993) reported the presence of a NPMF composed of cross-linked molecules containing multiple sulfur atoms, which represented up to 32 wt% of the whole material (Adam et al., 1992; Jenisch-Anton et al., 1999). Significantly different average molecular weight values of NPMF from RP oil were reported using various techniques (Adam et al., 1993): 815 Da by vapor pressure osmometry; 3400 Da by light scattering measurements and 1660 Da by size exclusion chromatography.

Despite a minor clean-up of non-S-bearing heteroatom classes that was applied during sample preparation, FTICR-MS spectra of NPMF fractions of JH and RP oils analyzed in this study are very similar to the respective whole oil spectra (compare panels A vs. B and C vs. D in Fig. 1),

299 indicating that the analyses of whole oils by (+) APPI are representative and capture the major S-
300 bearing constituents in those oils.

301 The spectra shown in Fig. 1 (A-G) revealed no detectable peaks above *m/z* 1100 in all the
302 analyzed oils and fractions. To further corroborate the absence of high molecular weight
303 compounds, we focused on the well-studied RP oil as representing very low maturity, high sulfur
304 oils. A (+) APPI FTICR mass spectrum was collected from *m/z* 1000–3000 (Fig. 1H), after
305 tuning the instrument with Agilent Low Concentration Tuning mix for enhanced sensitivity at
306 this *m/z* range. A group of peaks was detected in the RP oil at *m/z* 1000-1250 in Fig. 1H. Yet, no
307 evidence could be found for larger molecules (*m/z* > 1500). If the NPMF is formed by
308 consecutively adding building block units in a process similar to vulcanization, fragments at *m/z*
309 > 1250 would be expected since a continuum of species should exist (Eglinton et al., 1994). The
310 Jianghan and Rozel Point oil NPMF spectra (Fig 1B and 1D, respectively) showed no indication
311 of 'macromolecules' in their composition. Notably, there is no evidence of in-source
312 fragmentation, consistent with previous work by Bagag et al. (2008) on the APPI analysis of
313 sensitive biomolecules, nor evidence of fragmentation during the ion transfer to the ICR cell. In
314 addition, the samples fully dissolved in toluene and no evidence of molecular aggregation was
315 seen visually or in the mass spectra. Hence, the (+) APPI FTICR-MS spectra obtained herein
316 represent a key piece in the understanding of the so called NPMF. The (+) APPI FTICR-MS
317 results clearly indicate that a macromolecular fraction >1250 Da is not present in the RP and JH
318 oils.

319 Intermolecular sulfur incorporation is inferred from the elevated relative intensity detected in the
320 $C_{54\text{-}59}$ range within class $S\bullet_1$ DBE 8 (Fig. 8), tentatively interpreted to be the indication of two
321 $C_{27\text{-}29}$ steroidal units bridged by one sulfur atom, each unit contributing 4 double bond
322 equivalents. Noteworthy, a similar pattern was seen in class $S\bullet_{2\text{-}3}$ DBE 9-11 $C_{54\text{-}59}$ species, but
323 not in class $S\bullet_1$ DBE 7, which further suggests these species are indeed two bridged steroid units
324 (no DBE < 8) or eventually hopanoids for species with higher DBE. RP class $S_2\bullet$ DBE 11 $C_{56\text{-}57}$
325 compounds were selected as targets for CID experiments (Table 3) and results show detectable
326 daughter ions with the loss C_{28} and C_{29} with no sulfur and ΔDBE of 5.5, suggestive of an
327 intermolecular linkage.

Although they were inferred to exist, intermolecular sulfur incorporation reactions that yield high molecular weight molecules are limited. Recent investigations have recognized the impact of nanoaggregation on molecular weight measurements of other oil components, such as asphaltenes (Zhang et al., 2013). Initially thought to be as high as several thousand kilodaltons, the average molecular weights of non-aggregated asphaltene distributions are now recognized to be around 750 Da (Mullins, 2010; Hosseini-Dastgerdi et al., 2015; Snowdon et al., 2016). Similarly, an eventual aggregation of sulfurized species might be the reason for the overestimation of NPMF molecular weights as measured via light scattering and size exclusion chromatography in previous studies (Adam et al., 1993).

4.2. Thermally immature vs. biodegraded sulfur rich oils

Sinninghe Damsté and De Leeuw (1987) used gas chromatography coupled to mass spectrometry (GC-MS), to identify not only sulfur containing isoprenoids (C_{15} and C_{20}) in Rozel Point oils but also a series of isoprenoid chains bonded to several organosulfur structures (e.g. thiophenes, thiolanes, benzothiophenes). Further work led by the same authors expanded the scope of sulfur compounds detected by GC-MS: C_{30} and C_{35} isoprenoid thiophenes, alkylthianes, isoprenoid thiolanes, thiophene steranes, thiolane steranes, alkylbenzothiophenes, isoprenoid benzothiophenes, isoprenoid bithiophenes and sulfur-containing hopanoids. In total, around one thousand sulfur compounds were identified, with a molecular weight upper limit of 600 Da and a maximum of two sulfur atoms in the structure (Sinninghe Damsté et al., 1987). Such species were considered different from those sulfur compounds found in most oils since their structures are closely related to biogeochemical precursors (Sinninghe Damsté et al., 1989). Lu et al. (2014) investigated a set of Jianghan oils using (+) ESI FTICR-MS, after S-methylation reactions and detected high levels of alkylcyclothioethers within the oils. The identified peaks ranged from classes $S_{1\text{-}3}$, DBE 1-14, and $C_{10\text{-}35}$. Lu et al. (2014) also showed that compounds from class S_1 DBE 1-3 were detected with remarkably higher relative intensities and the predominance of $C_{20\text{-}21}$ compounds was attributed to the sulfurization of phytanic acids and phytols, and the overall sulfurization mechanism in Jianghan oils was hypothesized to involve carboxylic acids and fatty alcohols, which resulted in the formation of cyclic thioethers. Kohnen et al. (1993) identified sulfur-bound steroid and phytane moieties in the Jianghan oil (also in Rozel Point oil), suggesting that di- or polysulfide linkages are present in S-containing moieties and the position

of double bonds in the precursors controls the position of S-linkages. Liu et al. (2018) showed that the ubiquitous sulfur ring structures present in the organic sulfur compounds in Jianghan Basin oils likely originated from intramolecular sulfurization reactions.

The biogeochemistry of Peace River oils has been extensively studied in our group by Adams et al. (2013) and Bennett et al. (2013). More recently, Oldenburg et al. (2017) have shown the effects of different biodegradation levels in the chemical composition distribution in a Peace River area, Bluesky Formation reservoir profile, as measured by FTICR-MS. Overall, molecules with higher DBE and higher sulfur number were found to be more resistant to biodegradation.

The results of this study show that the mass spectra of Jianghan and Rozel Point oils are remarkably different from the spectra of the Peace River oils (Fig. 1, A and C vs. E – G). The smoother distribution of peaks detected in the Peace River oils, similar to a bell-shaped curve, is a very common observation in fossil fuel analysis (Marshall and Rodgers, 2008) and relates to the loss of carbon number preferences caused by the thermal cracking of kerogen during oil generation. On the other hand, both Jianghan and Rozel Point oils show mass spectra that reflect a dominant signature of precursor compounds (Fig. 3C), somewhat akin to the spectra observed in recent marine sediments (Radović et al., 2016a), a consequence of the low thermal stress levels experienced by these oils. Thus, both Rozel Point and Jianghan oil (+) APPI FTICR-MS mass spectra are a good representation of the chemical species and mechanisms involved in early diagenesis and related sulfur incorporation processes.

In these two oils, the predominance of heteroatom classes with one or more sulfur atoms (S_{1-6}) is remarkable (Fig. 2), whereas classes HC, O_{1-2}, and NO_{0-1} are the only non-sulfur containing heteroatom classes detected, accounting in total for less than 10% relative intensity in JH and RP oils. The vast majority of compounds detected in these low maturity oils are sulfurized. In addition, this is the first report of species with more than two sulfur atoms per molecule in Rozel Point oils, while Liu et al. (2018) detected up to S_5 compounds in Jianghan oils.

The Peace River oils exhibit higher relative intensity for S_1• species, and a lower relative intensity as the sulfur number increases up to S_4• (Fig. 3A). Both Rozel Point and Jianghan oils, on the other hand, show maximum relative intensity at S_2• and extend up to S_6• and S_5•, respectively. Such differences may be associated with the depositional settings favoring organic

matter reaction with one or more sulfide species, coupled to the low thermal stress experienced by the Jianghan and Rozel Point oils. Therefore, the relative ratios of lesser and more extensively sulfurized compound classes (e.g. S_1• vs. S_2•) is proposed as a proxy for source rock depositional settings, although further testing with an extended sample set is required.

Peace River oils WC and BS show very similar chemical composition (Figs. 2 and 3). Despite showing a similar carbon number distribution to its Peace River analogs in Fig. 3C, the Peace River GR oil DBE distribution is significantly shifted towards lower DBE values (Fig. 3B), while exhibiting a relative enrichment in S_2• species (Fig. 3A). Geochemical differences among the Peace River oils studied herein have been observed before by Adams et al. (2013), including a lower thermal maturity, lower biodegradation extent and higher sulfur content for oils primarily sourced from the sulfur enriched Gordondale Formation.

4.3. Sulfurized steroids and hopanoids (class S_1• DBE 5-6)

In a study by Lu et al. (2013), C_{28-30} DBE 5-7 steroids were detected in class S_1 of a sulfur rich heavy oil in Jiaxian Sag, Bohai Bay Basin, China. Sulfurized steroidal structures were previously reported in RP oil as part of the macromolecular matrix through a sulfur linkage located in ring A or B (Adam et al., 1992). Thiophene and thiolane steranes have been identified in RP oil by Sinninghe Damsté et al. (1987). Using selective cleavage of acyclic sulfide by superheated methyl iodide, Schouten et al. (1993) described the release of C_{27-30} steroid products from RP polar and asphaltene fractions. Kohnen et al. (1993) suggested that multiple substrates prone to sulfur incorporation reactions, such as Δ2-, Δ3-, Δ5-sterenes or Δ3,5-steradienes, give rise to a large variation in the positions and stereochemistry of sulfur incorporated steroids and that timing of sulfur incorporation during diagenesis would significantly influence the resulting products.

As can be observed in both in the overall (Fig. 3B) and class S_1• (Fig. 4A) DBE number distribution plots, there is an elevated relative intensity of DBE 5-6 species in Rozel Point and Jianghan oils. C_{27-30} species largely dominate the class S_1• DBE 5 carbon number distribution (Fig. 5A). Since DBE 4 species do not show an elevated relative intensity for C_{27-30} in any compound classes (except for HC•), sulfurized steroid-like compounds likely include a cyclothioether moiety to result in a DBE 5 value (Fig. 5A). Although present, C_{27-30} species do

not exhibit an elevated relative intensity within heteroatom classes with more than 2 sulfur atoms. This suggests that less functionalized molecular precursors such as steroids yield less sulfurized diagenesis products, in contrast to precursors such as carotenoids that have multiple reactive sites for sulfur incorporation (Section 4.5).

Results also suggest the occurrence of sulfurized homohopanes and norhopanes. The prominent class S_1• DBE 6 C_{35} peak (Fig. 5B) may represent the sulfurized analog of C_{35} homohopanes, which are known to be the dominant triterpene in the Rozel Point oil. The elevated relative intensity of class S_1• DBE 6 $C_{27\text{-}29}$ species in RP oil is remarkable (Fig. 5B) because there have been no reports of S-bound norhopanes despite the occurrence of S-bound (homo)hopanes in thermally immature sedimentary organic matter. Within the most plausible routes for the production of sulfurized steroids in natural environments (Lu et al., 2013), none would yield S-steroid species with DBE 6. To further investigate the forgoing interpretations, ions from class S_1• DBE 5 $C_{27\text{-}30}$ were selected as targets for CID experiments (Table 2). In both RP and JH oils, detected daughter ions represent the loss of $C_{1\text{-}6}$ fragments with ΔDBE -0.5, i.e. aliphatic moieties such as -CH_3, -C_2H_5, and no sulfur atoms, compatible with a side carbon chain fragmentation from a D-ring or an AB-ring sulfurized steroid (Lu et al., 2013). The RP oil targeted ions show, although with low relative intensity, $\Delta C_{0\text{-}2}\ \Delta S_1$ daughter ions, which indicate that some class S_1• DBE 5 $C_{27\text{-}30}$ isomers might have thiol ($\Delta C_0\ \Delta S_1$ fragments) or aliphatic sulfide ($\Delta C_{1\text{-}2}\ \Delta S_1$) as functional groups, instead of cyclic sulfide. In such cases, the parent DBE 5 ion could represent, among other structures, either a 5-ring moiety (e.g., hopanoids) or a 4-ring structure with one carbon-carbon double bond (e.g., sterenes). However, to the best of our knowledge, no sterenes have been detected in RP oil, despite being thermally immature, thus the occurrence of sulfurized norhopanes as class S_1• DBE 6 $C_{27\text{-}29}$ species is more likely.

4.4. Class S_1 DBE 1 and class S_1• DBE 3 species

Previous work by Lu et al. (2014) indicated that the Jianghan oils are relatively enriched in Class S_1 DBE 1-3 species, and the same pattern was observed herein (Figs. 4A,B). The elevated relative intensity of class S_1 DBE 1 species suggests an enrichment in thiolanes or thianes, whereas elevated relative intensity of class S_1• DBE 3 species suggests thiophenic structures. There is an even/odd predominance spanning $C_{16\text{-}40}$ class S_1 DBE 1 species in Jianghan oil (Fig.

6A). Lu et al. (2014) reported the occurrence of odd/even predominance in the Jianghan oil class S_1, centered around the C_{21} peak. Although not discussed in their paper, the methylation reactions used by Lu et al. (2014) to facilitate (+) ESI detection of sulfur species added one carbon to all the species detected in their study, and this might have caused the reversal of actual even/odd carbon preference to observed odd/even preference in their data. In agreement with our observations, Sinninghe Damsté et al. (1987) and Sheng et al. (1987) reported a series of $C_{10\text{-}32}$ alkylthiolanes and alkylthianes in Rozel Point and Jianghan oils, respectively, which also exhibited a strong even/odd preference. Here, the (+) APPI results show that the even/odd preference extends much further, up to C_{40} in the Jianghan oil (Fig. 5A).

CID experiments were also performed to investigate the fragmentation patterns of class S_1 DBE 1 $C_{26,28,30}$ species. However, the experiments failed to produce any detectable daughter ion at *m/z* > 150. Typically, CID promotes the rupture of the weakest bonds in a molecule, therefore the intermediate species generated after C-S bond cleavage in thiolanes/thianes might have undergone extensive fragmentation. Based on the same reasoning, the presence of aliphatic thiols or dialkylsulfides contributing to class S_1 DBE 1 species cannot be precluded, although the lack of class S_1 DBE 0 species indicates such functional groups may be largely absent in the oil matrices. Initially thought as intermediates in the formation of thiophenes, thiolanes have been detected in sediment extract but their association with thiophene formation remains unclear (Sinninghe Damsté et al., 1986). The (+) APPI FTICR-MS results support the hypothesis that (a) these cyclic sulfides, formed during very early stages of diagenesis, likely never partake in the kerogen formation (Brassell et al., 1988; Peng et al., 1998); and that (b) these cyclic sulfides may be derived from the same functionalized precursors as the *n*-alkanes, such as *n*-alkanoic acids and *n*-alkanols (Brassell et al., 1988; Liu et al., 2018). In this sense, reasonable follow up research might incorporate a comprehensive assessment of sulfur-bearing species in sediment extracts, occurring throughout a thermal maturity sequence, from recent immature sediments to Type IIS kerogen at ~0.6 %Ro, to get insights on the dynamics of free molecules versus those that are bound-then-released from kerogen.

Class S_1• DBE 3 species, which putatively represent thiophenic structures, show elevated relative intensity at $C_{20,30,35,40,45}$ in the Rozel Point oil, and at $C_{20,24\text{-}26,28,30,40}$ in the Jianghan oil (Fig. 5B). FTICR-MS data alone are not capable of distinguishing isomers, but the elevated relative

intensity of multiple isoprene units (x*C_5 units) may indicate the detection of an extended range of isoprenoid thiophenes. To support this reasoning, isoprenoid thiophenes with < 35 carbons have been identified by GC-MS in Rozel Point and Jianghan oils, as reported by Sinninghe Damsté et al. (1987) and Sheng et al. (1987), respectively.

4.5. C_{40} species

The overall carbon distribution plot (Fig. 3C) shows an elevated relative intensity for C_{40} species in both RP and JH oils. This observation alone suggests the presence of compounds bearing much of the carbon skeleton from their biological precursor. Carotenoids are the likely biological source for C_{40} species, since they are common constituents of living organisms with wide taxonomic diversity, from archaea and cyanobacteria to higher plants and animals (Walter and Strack, 2011). Recently, we used a similar (+) APPI FTICR-MS approach to characterize carotenoids in recent marine sediments, in addition to various other lipid markers (Radović et al., 2016a). Whereas $C_{27\text{-}30}$ S-bearing steroids appear to be limited to classes $S_{1\text{-}2}$ (see Section 4.3.), C_{40} S-carotenoids are seen in classes with up to six sulfur atoms. Such findings indicate the clear dependence of the degree of sulfur incorporation on the number of double bonds present in the lipid undergoing diagenesis, supporting the observations and interpretations reported previously with ESI FTICR-MS data (Liu et al., 2018). Amrani and Aizenshtat (2004) highlighted the importance of carbonyl groups for the sulfurization processes in marine sediments, but the C_{40} S-carotenoid species suggested here indicate that carbon-carbon double bonds may be driving the sulfurization in such species. Carotenoids can offer multiple spots for sulfur incorporation, contrary to steroids which have a limited number of double bonds and oxygenated groups. The predominance of C_{40} in classes $S_{5\text{-}6}$• is remarkable and reveals that, overall, most of the sulfurized species may resemble the biological precursors in both Jianghan and Rozel Point oils. Further comparisons between sulfurization reactions in the laboratory versus natural settings with various precursor molecules are required.

Typical carotenoid structures (e.g., lycopene, β-carotene, nostoxanthin) have 13 DBE units, although higher DBE species are also possible (Walter and Strack, 2011). Carotenoid diagenesis in different depositional settings can be quite complex (Watts and Maxwell, 1977; Repeta and Gagosian, 1987), but the identification of several reduced carotenoids in recent sediments

suggests that hydrogenation occurs during diagenesis without structural or stereochemical specificity (Hebting et al., 2006). Adam et al. (1993) not only suggested acyclic carotenes, β-carotene and monocyclic carotenes as building blocks of Rozel Point NPMF, but also discussed their implications to organic matter input determination. In the current study, similarly to Liu et al. (2018), sulfurized carotenoids are present in the oils as free molecules instead of being building blocks of NPMF, as evident by the absence of cross-linked carotenoid-derived NPMF intermediates (i.e., no significant signal from C_{80} species was detected). In summary, the sulfur incorporation in carotenoid precursors is not followed by an increase in the carbon number, thus mostly original (biological) C_{40} species with varying DBE values were detected.

Fig. 7 shows the DBE distribution of classes $S_{1\text{-}5}$• C_{40} species. A significant intraclass pattern observed in Fig. 7 is the elevated relative intensity for the DBE = S + (2,4,6) species, which might reflect the level of 'thiophenization'. That is, DBE = S + 0 species would represent altered aliphatic carotenoids (e.g. lycopene) where the sulfur atoms are incorporated as thiolane. DBE = S + 2 species represent the altered carotenoids with 2 cyclic structures (e.g., beta-carotane) where sulfur atoms are incorporated as thiolane. Note the higher relative intensity of DBE S + 2 compared to DBE S + 0 species, reflecting the higher abundance of cyclic carotenoid structure in the deposited organic matter. Since the conversion of a thiolane into thiophenes involves a ΔDBE +2 shift, species with DBE S + 4 and S + 6 may reflect the number of thiophenic structures present in the compound. The transformation of thiolanes into thiophenes is likely dependent on the thermal stress level experienced by the sample. The ratios of thiophene and thiolane structures within the carotenoid classes require further investigation to determine its potential usefulness as a marker for early diagenesis sulfurization.

4.6. The DBE number ≥ S_x rule

In Fig. 7, the minimum detected DBE number in each plot is equal to the number of sulfur atoms of the corresponding class, i.e. DBE number ≥ S_x, which indicates that, for C_{40} assignments, the sulfur incorporation reactions are associated with a DBE increase. In fact, such a pattern is observed in the dominant molecular formulae detected in this study, indicating that polysulfides, aliphatic sulfides and thiols must be largely absent as stand-alone functional groups in the RP and JH oils. The only exceptions to the rule are class S_2• DBE 1 $C_{16,18,20,22,24,26}$ and class S_3• DBE

2 C_{37} species. The even/odd predominance in class S_1 DBE 1 was discussed previously. The species in class S_2• DBE 1 $C_{16,18,20,22,24,26}$ probably relates to those where an additional sulfur atom is incorporated as a cyclic polysulfide or a thiol. The class S_3• DBE 2 C_{37} species are discussed in Section 4.7.

4.7. Sulfurized alkenones

Alkenones are long chain unsaturated ketones produced by some phytoplankton species and typically used as paleoenvironmental proxies (Volkman et al., 1980; Brassell et al., 1986). An elevated relative intensity was observed for classes $S_{1\text{-}3}$• DBE 1-3 C_{37} species in Rozel Point oil, suggesting that alkenones have also undergone sulfurization during diagenesis. Although it is tempting to try and estimate the ratios of parent $C_{37:2}$ and $C_{37:3}$ (e.g., $U_{37}^{K'}$) based on their sulfurized analogs, this exercise would be highly speculative at this point. Also, the occurrence of class S_3• DBE 2 C_{37} species as an exception to the DBE number $\geq S_x$ rule, indicates that in some cases thiol or polysulfides might be present. The peak representing class S_2• DBE 2 C_{37} in Rozel Point oil was selected for CID experiments, and similarly to class S_1 DBE 1 peaks, no daughter ions could be detected, except for an ion representing the loss of a -SH group, although results do not clarify where this functional group occurs in the alkenone molecules. This result suggests that the C_{37} assignments investigated herein may display long alkyl chains that, in turn, produce daughter ions, which undergo further fragmentation outside of our analytical window at *m/z* >150.

4.8. Implications for atmospheric carbon dioxide removal

To meet the challenges of climate predictions at the end of the 21st century (IPCC, 2018), technologies will be needed that remove carbon dioxide from the atmosphere and sequester it for geological time frames. Such processes, termed carbon dioxide removal (CDR) are increasingly attracting both research and commercial investment interest. Only a few CDR technologies are currently being commercially developed (e.g., bio-energy with carbon capture and storage, or direct air capture), but are still far below the scale needed for globally significant CO_2 reduction, which would require achieving carbon drawdowns in the order of 100 to 1000 Gt/y by the year 2100 (IPCC, 2018). A better understanding of natural mechanisms for long term preservation of organic molecules can provide guidelines for the development of technologies that could

leverage those mechanisms to artificially enhance the removal of carbon in the geosphere in the form of engineered organic species. We term these species "alternative vectors for carbon storage", or AVECS for short, and are currently investigating several routes to produce AVECS from organic precursors, including pathways involving sulfurization of organic molecules (Yim, 2019). In one of the concepts under investigation, waste biomass and sulfur, which is a by-product of sour petroleum production, are the feedstocks for a long-term subsurface preservation of organic carbon in the geosphere. To that end, the study reported herein provided multiple indications relevant to AVECS technology development issues such as:

- Natural precursors such as pigments or lipids can incorporate sulfur as free molecules;
- Double bonds are the key molecular site for sulfur incorporation;
- Given the fact that double bonds are quite reactive, the sulfur incorporation must be taking place early in the diagenesis, at low pressures and temperatures, which favorably implies fewer energy needs for AVECS production;
- Cyclization is the favored sulfur incorporation mechanism producing thiolane structures, which can then be aromatized to thiophenes during diagenesis.

Some of these processes can be modelled and reproduced in the laboratory (Yim, 2019), however much more research effort will be needed to move these types of reactions from bench-scale to sustainable pilot or large-scale deployments; notwithstanding, biogeochemical processes occurring in geosphere, such as those inferred from the current study of sulfur rich oils, can provide valuable insights and lessons that can direct this type of research.

5. Conclusions

The present study leveraged the expanded analytical window offered by novel analytical technologies to improve the current geochemical understanding of diagenetic processes involving sulfur and the resultant occurrence of sulfur rich oils. A set of five sulfur rich oils was analyzed via (+) APPI FTICR-MS and CID-FTICR-MS. From these results, we conclude:

The absence of peaks at $m/z > 1250$ in Rozel Point and Jianghan oils, in their non-polar macromolecular fractions does not support the concept of a macromolecular network linked by (poly)sulfide bridges that was proposed to explain the occurrence of non-GC-MS amenable sulfur

compounds in immature, sulfur rich oils. Instead, it appears that the presence of highly sulfurized lipids (up to six sulfur atoms) as free molecules are the result of sulfurization with the degree of sulfur incorporation dependent on the abundance of functional groups (double bonds mainly) in the precursor molecules.

Source rock thermal stress levels were found to be a key factor differentiating the composition of biodegraded, sulfur-rich Peace River oils, compared to thermally immature, sulfur-rich Rozel Point and Jianghan oils. Whereas Peace River oils do not show biological precursor skeleton signatures, Rozel Point and Jianghan oils show the presence of S-containing steroids, hopanoids, carotenoids and alkenones among others.

(+) APPI CID-FTICR-MS experiments indicated only a minor occurrence of thiol functional groups and sulfide bridges linking two precursor molecules. The compositional patterns observed in sulfurized C_{40} assignments, representing S-bound carotenoids, supports a mechanism of sulfur incorporation involving the formation of thiolane structures (and to a lesser extent, thianes), which can then be aromatized to thiophenes during diagenesis. CID-FTICR-MS experiments were also helpful to prove the occurrence of intermolecular sulfur incorporation reactions as a secondary mechanism, the aliphatic nature of class S_1 DBE 1 species and sulfurized alkenones, the preference of cycle-forming sulfur incorporation in steroid structures, and the occurrence of thiol/thioether groups, although these were seen only to a minor extent.

The analytical approach presented here can be improved and expanded using analytical workflows that include chromatographic separation to better characterize individual molecular species, as well as by studying other sample types such as source rocks and recent sediments to better constrain the progression of diagenetic processes involving sulfur incorporation.

The occurrence of S-bound compounds in oils or sediment extracts, as detected via FTICR-MS, can be used as proxies for depositional environment, organic matter input, sulfurization and other diagenetic processes. Understanding the relationship between the precursor and sulfurized products, as well as the mechanisms for such reactions, is key to the design of geoengineering solutions to enhance carbon preservation in the geosphere by promoting sulfurization of biomass.

AUTHOR INFORMATION

Corresponding author

*Telephone: +1 403 210.3916. Fax: +1 403 220.8618. E-mail: rcsilva@ucalgary.ca

Notes

The authors declare no competing financial interest.

ACKNOWLEDGEMENTS

This research was made possible in part by research support from Canada First Research Excellence Fund (CFREF), UCalgary Global Research Initiative in Low Carbon Unconventional Resources, Foundation for Innovation (CFI), the Natural Sciences and Engineering Research Council of Canada (NSERC), PRG and the University of Calgary. Aphorist Inc. and Ryan W. Snowdon are acknowledged for software support.

This study was conceived of and designed by RCS, CY and SRL with key input from JRR and TBPO. CY carried out literature reviews, laboratory experiments, data interpretation and contributed to writing. FTICR-MS method optimization and analyses were carried out by MB, and data processing and interpretation were carried out by RCS. PW assisted with the NPMF fractionation. JRR contributed to data interpretation and manuscript writing. HH, LRS and TBPO assisted with sample collection and geochemical discussions on the petroleum systems aspects and prior FTMS studies of high sulfur oils. All authors revised the manuscript.

The manuscript benefited greatly from insightful contributions made by Morgan Raven and one anonymous reviewer. Clifford Walters (Associate Editor) is also acknowledged for suggesting edits that have improved the revised manuscript.

References

Adam, P., Mycke, B., Schmid, J.C., Connan, J., Albrecht, P., 1992. Steroid moieties attached to macromolecular petroleum fraction via di- or polysulphide bridges. Energy & Fuels 6, 553-559.

Adam, P., Schmid, J.C., Mycke, B., Strazielle, C., Connan, J., Huc, A., Riva, A., Albrecht, P., 1993. Structural investigation of nonpolar sulfur cross-linked macromolecules in petroleum. Geochimica et Cosmochimica Acta 57, 3395-3419.

Adams, J., Larter, S., Bennett, B., Huang, H., 2012. Oil charge migration in the Peace River oil sands and surrounding region. Abstract. GeoConvention 2012: Vision, Calgary.

Adams, J., Larter, S., Bennett, B., Huang, H., Westrich, J., & Kruisdijk, C. v. 2013. The dynamic interplay of oil mixing, charge timing, and biodegradation in forming the Alberta oil sands: Insights from geologic modeling and biogeochemistry, In: Hein, F. J., Leckie, D., Larter, S., Suter, J. R. (Eds.), Heavy-Oil and Oil-Sand Petroleum Systems in Alberta and Beyond. American Association of Petroleum Geologists, pp. 23-102

Aizenshtat, Z., Krein, E.B., Vairavamurthy, M.A., Goldstein, T.P., 1995. Role of Sulfur in the Transformations of Sedimentary Organic Matter: A Mechanistic Overview, in: Geochemical Transformations of Sedimentary Sulfur, ACS Symposium Series. American Chemical Society, pp. 2–16.

Allan, J., Creaney, S., 1991. Oil families of the Western Canada Basin. Bulletin of Canadian Petroleum Geology 39, 107-122.

Amrani, A. and Aizenshtat, Z., 2004. Mechanisms of Sulfur Introduction Chemically Controlled: $\delta^{34}S$ Imprint. Organic Geochemistry, 35, 1319-1336.

Amrani, A., 2014. Organosulfur compounds: Molecular and isotopic evolution from biota to oil and gas. Annual Review of Earth and Planetary Sciences 42, 733-768.

Bagag, A., Giuliani, A., Laprévote, O., 2008. Atmospheric pressure photoionization mass spectrometry of oligodeoxyribonucleotides. European Journal of Mass Spectrometry 14, 71-80.

Bennett, B., Adams, J.J., Gray, N.D., Sherry, A., Oldenburg, T.B.P., Huang, H., Larter, S.R., Head, I.M., 2013. The controls on the composition of biodegraded oils in the deep subsurface – Part 3. The impact of microorganism distribution on petroleum geochemical gradients in biodegraded petroleum reservoirs. Organic Geochemistry 56, 94-105.

Brassell, S.C., Eglinton, G., Marlowe, I.T., Pflaumann, U., Sarnthein, M., 1986. Molecular stratigraphy: A new tool for climatic assessment. Nature 320, 129-133.

Brassell, S.C., Eglinton, G., Sheng, G., Fu, J., 1988. Biological markers in lacustrine Chinese oil shales. In: Fleet, A.J., Kelts, K., Talbot, M.R. (Eds.) Lacustrine Petroleum Source Rocks Geological Society Special Publication 40, 299-308.

Carroll, A., Bohacs, K., 2001. Lake-type controls on petroleum source rock potential in nonmarine basin. American Association of Petroleum Geologists Bulletin 85, 1033-1053.

Eglinton, T.I., Irvine, J.E., Vairavamurthy, A., Zhou, W., Manowitz, B., 1994. Formation and diagenesis of macromolecular organic sulfur in Peru margin sediments. Organic Geochemistry 22, 781-799.

Hansell, D.A., Carlson, C.A., Repeta, D., Schlitzer, R., 2009. Dissolved organic matter in the ocean: New insights stimulated by a controversy. Oceanography 22, 202-211.

Hebting, Y., Schaeffer, P., Behrens, A., Adam, P., Schmitt, G., Schneckenburger, P., Bernasconi, S.M., Albrecht, P., 2006. Biomarker evidence for a major preservation pathway of sedimentary organic carbon. Science 312, 1627-1631.

Hosseini-Dastgerdi, Z., Tabatabaei-Nejad, S.A.R., Khodapanah, E., Sahraei, E., 2015. A comprehensive study on mechanism of formation and techniques to diagnose asphaltene structure; molecular and aggregates: A review. Asia-Pacific Journal of Chemical Engineering 10, 1-14.

Hou, Y., Wang, F., He, S., Dong, T., Wu, S., 2017. The properties and shale oil potential of saline lacustrine shales in the Qianjiang Depression, Jianghan Basin, China. Marine and Petroleum Geology 86.

Houghton, R.A., 2007. Balancing the global carbon budget. Annual Review of Earth and Planetary Sciences 35, 313-347.

Huang, C., Hinnov, L., 2014. Evolution of an Eocene-Oligocene saline lake depositional system and its controlling factors, Jianghan Basin, China. Journal of Earth Science 25, 959-976.

Hughey, C.A., Rodgers, R.P., Marshall, A.G., Walters, C.C., Qian, K., Mankiewicz, P., 2004. Acidic and neutral polar NSO compounds in Smackover oils of different thermal maturity revealed by electrospray high field Fourier transform ion cyclotron resonance mass spectrometry. Organic Geochemistry 35, 863-880.

IPCC, 2018. Global Warming of 1.5° C: An IPCC Special Report on the Impacts of Global Warming of 1.5° C Above Pre-industrial Levels and Related Global Greenhouse Gas Emission Pathways, in the Context of Strengthening the Global Response to the Threat of Climate Change, Sustainable Development, and Efforts to Eradicate Poverty. Intergovernmental Panel on Climate Change. Masson-Delmotte, V. Zhai, P. Pörtner, H.O. Roberts, D. Skea, J., Shukla, P.R., Pirani, A., Moufouma-Okia, W., Péan, C., Pidcock, R., Connors, S., Matthews, J.B.R., Chen, Y., Zhou, X., Gomis, M., Lonnoy, E., Maycock, T., Tignor, M,. Waterfield, T. (Eds.) SR15.

Jenisch-Anton, A., Adam, P., Schaeffer, P., Albrecht, P., 1999. Oxygen-containing subunits in sulfur-rich nonpolar macromolecules. Geochimica et Cosmochimica Acta 63, 1059-1074.

Jiao, N., Herndl, G.J., Hansell, D.A., Benner, R., Kattner, G., Wilhelm, S.W., Kirchman, D.L., Weinbauer, M.G., Luo, T., Chen, F., Azam, F., 2010. Microbial production of recalcitrant dissolved organic matter: Long-term carbon storage in the global ocean. Nature Reviews Microbiology 8, 593-599.

Kilgour, D.P.A., Neal, M.J., Soulby, A.J., O'Connor, P.B., 2013. Improved optimization of the Fourier transform ion cyclotron resonance mass spectrometry phase correction function using a genetic algorithm. Rapid Communications in Mass Spectrometry 27, 1977-1982.

Kohnen, M.E.L., Sinninghe Damsté, J.S., Baas, M., Dalen, A.C.K., de Leeuw, J.W., 1993. Sulphur-bound steroid and phytane carbon skeletons in geomacromolecules: Implications for the mechanism of incorporation of sulphur into organic matter. Geochimica et Cosmochimica Acta 57, 2515–2528.

Liu, W., Liao, Y., Shi, Q., Hsu, C.S., Jiang, B., Peng, P.a., 2018. Origin of polar organic sulfur compounds in immature crude oils revealed by ESI FT-ICR MS. Organic Geochemistry 121, 36-47.

Lu, H., Peng, P., Hsu, C.S., 2013. Geochemical explication of sulfur organics characterized by Fourier transform ion cyclotron resonance mass spectrometry on sulfur-rich heavy oils in Jinxian Sag, Bohai Bay Basin, northern China. Energy & Fuels 27, 5861-5866.

727 Lu, H., Shi, Q., Ma, Q., Shi, Y., Liu, J., Sheng, G., Peng, P., 2014. Molecular characterization of
728 sulfur compounds in some specieal sulfur-rich Chinese crude oils by FT-ICR MS. Science
729 China Earth Sciences 57, 1158-1167.
730 Marshall, A.G., Rodgers, R.P., 2008. Petroleomics: Chemistry of the underworld. Proceedings of
731 the National Academy of Sciences 105, 18090-18095.
732 Meissner, F.F., Woodward, J., Clayton, J.L., 1984. Stratigraphic relationships and distribution of
733 source rocks in the Greater Rocky Mountain Region. In: Woodward, J., Meissner, F.F.,
734 Clayton, J.L., (Eds.), Hydrocarbon Source Rocks of the Greater Rocky Mountain Region.
735 Rocky Mountains Assoc. Geol. pp. 1-34.
736 Mullins, O.C., 2010. The modified Yen model. Energy & Fuels 24, 2179-2207.
737 Oldenburg, T.B.P., Brown, M., Bennett, B., Larter, S.R., 2014. The impact of thermal maturity
738 level on the composition of crude oils, assessed using ultra-high resolution mass
739 spectrometry. Organic Geochemistry 75, 151-168.
740 Oldenburg, T.B.P., Jones, M., Huang, H., Bennett, B., Shafiee, N.S., Head, I., Larter, S.R., 2017.
741 The controls on the composition of biodegraded oils in the deep subsurface – Part 4.
742 Destruction and production of high molecular weight non-hydrocarbon species and
743 destruction of aromatic hydrocarbons during progressive in-reservoir biodegradation.
744 Organic Geochemistry 114, 57-80.
745 Orr, W.L., Sinninghe Damsté, J.S., 1990. Geochemistry of sulfur in petroleum systems. In: Orr.
746 W.L., White, C.M. (Eds.) Geochemistry of Sulfur in Fossil Fuels. ACS Symposium Series
747 429, American Chemical Society, pp. 2-29.
748 Peirong, W., Dajiang, Z., Guanjun, X., Tingrong, X., Fuqing, S., Bing, C., 2008. Geochemical
749 features of light hydrocarbons of typical salt lake oils sourced from Jianghan Basin, China.
750 Organic Geochemistry 39, 1631-1636.
751 Peng, P., Sheng, G., Fu, J., Wu, Z., Jiang, J., 1998. Origin of immature sulfur-rich oil in Jianghan
752 oil field. Chinese Science Bulletin 43, 678-681.
753 Philp, R.P., Zhaoan, F., 1987. Geochemical investigation of oils and source rocks from Qianjiang
754 depression of Jianghan Basin, a terrigenous saline basin, China. Organic Geochemistry 11,
755 549-562.
756 Pohlabeln, A.M., Gomez-Saez, G.V., Noriega-Ortega, B.E., Dittmar, T., 2017. Experimental
757 evidence for abiotic sulfurization of marine dissolved organic matter. Frontiers in Marine
758 Science 4, doi: 10.3389/fmars.2017.00364
759 Purcell, J.M., Hendrickson, C.L., Rodgers, R.P., Marshall, A.G., 2006. Atmospheric pressure
760 photoionization Fourier transform ion cyclotron resonance mass spectrometry for complex
761 mixture analysis. Analytical Chemistry 78, 5906-5912.
762 Radović, J., Silva, R., Snowdon, R., Brown, M., Larter, S.R., Oldenburg, T., 2016a. A rapid
763 method to assess a broad inventory of organic species in marine sediments using ultra-high
764 resolution mass spectrometry. Rapid Communications in Mass Spectrometry 30, 1273-
765 1282.
766 Radović, J.R., Silva, R.C., Snowdon, R., Larter, S.R., Oldenburg, T.B.P., 2016b. Rapid screening
767 of glycerol ether lipid biomarkers in recent marine sediment using atmospheric pressure
768 photoionization in positive mode Fourier transform ion cyclotron resonance mass
769 spectrometry. Analytical Chemistry 88, 1128-1137.
770 Raffaelli, A., Saba, A., 2003. Atmospheric pressure photoionization mass spectrometry. Mass
771 Spectrometry Reviews 22, 318-331.

772 Raven, M.R., Sessions, A.L., Adkins, J.F., Thunell, R.C., 2016. Rapid organic matter
773 sulfurization in sinking particles from the Cariaco Basin water column. Geochimica et
774 Cosmochimica Acta 190, 175-190.
775 Repeta, D.J., Gagosian, R.B., 1987. Carotenoid diagenesis in recent marine sediments—I. The
776 Peru continental shelf (15°S, 75°W). Geochimica et Cosmochimica Acta 51, 1001-1009.
777 Richnow, H.H., Jenisch, A., Michaelis, W., 1993. The chemical structure of macromolecular
778 fractions of a sulfur-rich oil. Geochimica et Cosmochimica Acta 57, 2767-2780.
779 Riediger, C., 1994. Migration of "Nordegg" Oil in the Western Canada Basin. How much and
780 how far? Bulletin of Canadian Petroleum Geology 42, 63-73.
781 Schouten, S., Pavlović, D., Sinninghe Damsté, J.S., de Leeuw, J.W., 1993. Selective cleavage of
782 acyclic sulphide moieties of sulphur-rich geomacromolecules by superheated methyl
783 iodide. Organic Geochemistry 20, 911-916.
784 Sheng, G., Fu, J., Brassell, S.C., Gowar, A.P., Eglinton, G., Sinninghe Damsté, J.S., de Leeuw,
785 J.W., Schenck, P.A., 1987. Sulphur-containing compounds in sulphur-rich crude oils from
786 hypersaline lake sediments and their geochemical implications. Chinese Journal of
787 Geochemistry 6, 115-126.
788 Sinninghe Damsté, J.S., De Leeuw, J.W., 1987. The origin and fate of isoprenoid C_{20} and C_{15}
789 sulphur compounds in sediments and oils. International Journal of Environmental
790 Analytical Chemistry 28, 1-19.
791 Sinninghe Damsté, J.S., De Leeuw, J.W., Kock-Van Dalen, A.C., De Zeeuw, M.A., Lange, F.D.,
792 Irene, W., Rijpstra, C., Schenck, P.A., 1987. The occurrence and identification of series of
793 organic sulphur compounds in oils and sediment extracts. I. A study of Rozel Point Oil
794 (U.S.A.). Geochimica et Cosmochimica Acta 51, 2369-2391.
795 Sinninghe Damsté, J.S., Rijpstra, W.I.C., De Leeuw, J.W., Schenck, P.A., 1989. The occurrence
796 and identification of series of organic sulphur compounds in oils and sediment extracts: II.
797 Their presence in samples from hypersaline and non-hypersaline palaeoenvironments and
798 possible application as source, palaeoenvironmental and maturity indicators. Geochimica et
799 Cosmochimica Acta 53, 1323-1341.
800 Sinninghe Damsté, J.S., ten Haven, H.L., De Leeuw, J.W., Schenck, P.a., 1986. Organic
801 geochemical studies of a Messinian evaporitic basin, northern Apennines (Italy)—II
802 Isoprenoid and *n*-alkyl thiophenes and thiolanes. Organic Geochemistry 10, 791-805.
803 Snowdon, L.R., Volkman, J.K., Zhang, Z., Tao, G., Liu, P., 2016. The organic geochemistry of
804 asphaltenes and occluded biomarkers. Organic Geochemistry 91, 3-15.
805 Summons, R., Amend, J., Bish, D., Buick, R., Cody, G., Des Marais, D., Dromart, G.,
806 Eigenbrode, J., Knoll, A., Sumner, D., 2011. Preservation of Martian organic and
807 environmental records: Final report of the Mars biosignature working group. Astrobiology
808 11, 157-181.
809 Tegelaar, E.W., de Leeuw, J.W., Derenne, S., Largeau, C., 1989. A reappraisal of kerogen
810 formation. Geochimica et Cosmochimica Acta 53, 3103-3106.
811 ten Haven, H.L., de Leeuw, J.W., Sinninghe Damsté, J.S., Schenck, P.A., Palmer, S.E.,
812 Zumberge, J.E., 1988. Application of biological markers in the recognition of
813 palaeohypersaline environments. In: Fleet, A.J., Kelts, K., Talbot, M.R. (Eds.) Lacustrine
814 Petroleum Source Rocks Geological Society, London, Special Publications 40, pp. 123-
815 130.
816 Vandenbroucke, M., Largeau, C., 2007. Kerogen origin, evolution and structure. Organic
817 Geochemistry 38, 719-833.

818 Volkman, J.K., Eglinton, G., Corner, E.D.S., Sargent, J.R., 1980. Novel unsaturated straight-
819 chain C_{37}-C_{39} methyl and ethyl ketones in marine sediments and a coccolithophore
820 *Emiliania huxleyi*. Physics and Chemistry of the Earth 12, 219-227.
821 Walter, M.H., Strack, D., 2011. Carotenoids and their cleavage products: Biosynthesis and
822 functions. Natural Product Reports 28, 663.
823 Walters, C.C., Qian, K., Wu, C., Mennito, A.S., Wei, Z., 2011. Proto-solid bitumen in petroleum
824 altered by thermochemical sulfate reduction. Organic Geochemistry 42, 999-1006.
825 Walters, C.C., Wang, F.C., Qian, K., Wu, C., Mennito, A.S., Wei, Z., 2015. Petroleum alteration
826 by thermochemical sulfate reduction – A comprehensive molecular study of aromatic
827 hydrocarbons and polar compounds. Geochimica et Cosmochimica Acta 153, 37-71.
828 Watts, C.D., Maxwell, J.R., 1977. Carotenoid diagenesis in a marine sediment. Geochimica et
829 Cosmochimica Acta 41, 493-497.
830 Werne, J.P., Hollander, D.J., Lyons, T.W., Sinninghe Damsté, J.S., Amend, J.P., Edwards, K.J.,
831 2004. Organic sulfur biogeochemistry: Recent advances and future research directions. In:
832 Amend, J.P., Edwards, K.J., Lyons, T.W. (Eds.) Sulfur Biogeochemistry - Past and
833 Present. GSA Special Papers 379, Geological Society of America, pp. 135-150
834 Yim, C. 2019. Organic Sulfur-Bearing Species as Subsurface Carbon Storage Vectors
835 (Unpublished master's thesis). University of Calgary, Calgary, AB.

836 Zhang, L., Shi, Q., Zhao, C., Zhang, N., Chung, K.H., Xu, C., Zhao, S., 2013. Molecular weight
837 and aggregation of heavy petroleum fractions measured by vapor pressure osmometry and
838 a hindered stepwise aggregation model. Energy & Fuels 27, 1331-1336.

839

840

841

842 **Table 1.** Sample codes and geochemical overview.

Code	Oil	Location	Sulfur (wt %)	Organic matter source	Depositional environment	Thermal maturity	Biodegradation	References
RP	Rozel Point	Utah, USA	9.4	Marine - lacustrine	hypersaline, lacustrine	Immature	Moderate	(Meissner et al., 1984; ten Haven et al., 1988; Sinninghe Damsté et al., 1989)
JH	Jianghan	Eastern China	5.6	Marine - lacustrine, with terrigenous inputs	hypersaline, lacustrine	Immature	Moderate	(Philp and Zhaoan, 1987; Carroll and Bohacs, 2001; Hou et al., 2017)
GR	Peace River	NW-Central Alberta, Canada	5.5	Marine - lacustrine, with terrigenous inputs	Marine - lacustrine	Mature - overmature	High	(Riediger, 1994; Adams et al., 2012; Adams et al., 2013; Bennett et al., 2013)
BS	Peace River	NW-Central Alberta, Canada	4.1	Marine - lacustrine	Marine - lacustrine	Mature - overmature	Very High	
WC	Peace River	NW-Central Alberta, Canada	4.2	Marine - lacustrine	Marine - lacustrine	Mature - overmature	High	

843

844

Table 2. (+) APPI CID-FTICR-MS results of class S_1 DBE 5 $C_{27\text{-}30}$ species. Relative intensities are normalized to the most intense daughter ion as the target peak is considered in the relative intensity calculations. Fragments with carbon or sulfur number higher than the parent peak, as well as those with relative intensity <10%, are not shown. Note: *lost of an even number of hydrogens, **fragment is likely not originated from the parent ion.

Parent	Oil	Fragment	Lost	Relative intensity (%)
$C_{27}H_{46}S$	Jianghan	$C_{26}H_{43}S$	$-CH_3$	100.0
		$C_{22}H_{35}S$	$-C_5H_{11}$	99.3
		$C_{24}H_{39}S$	$-C_3H_7$	40.7
		$C_{23}H_{37}S$	$-C_4H_9$	32.2
	Rozel Point	$C_{26}H_{43}S$	$-CH_3$	100.0
		$C_{22}H_{35}S$	$-C_5H_{11}$	84.9
		$C_{24}H_{39}S$	$-C_3H_7$	19.5
		$C_{23}H_{37}S$	$-C_4H_9$	16.2
		$C_{27}H_{45}$	-SH	15.5
		$C_{19}H_{29}S$	$-C_8H_{17}$	13.8
		$C_{26}H_{41}$	$-CH_5S$	12.9
		$C_{21}H_{34}S$	$-C_6H_{12}$*	12.3
		$C_{17}H_{26}S$	$-C_{10}H_{20}$*	10.2
$C_{28}H_{48}S$	Jianghan	$C_{27}H_{45}S$	$-CH_3$	100.0
		$C_{23}H_{37}S$	$-C_4H_9$	89.3
		$C_{22}H_{35}S$	$-C_5H_{11}$	76.1
		$C_{12}H_{15}S$	$-C_{16}H_{33}$	38.3
		$C_{25}H_{41}S$	$-C_3H_7$	31.2
		$C_{21}H_{33}S$	$-C_6H_{13}$	27.7
		$C_{24}H_{39}S$	$-C_4H_9$	26.5
	Rozel Point	$C_{27}H_{45}S$	$-CH_3$	100.0
		$C_{22}H_{35}S$	$-C_6H_{13}$	44.4
		$C_{23}H_{37}S$	$-C_5H_{11}$	41.7
		$C_{25}H_{41}S$	$-C_3H_7$	19.7
		$C_{21}H_{33}S$	$-C_7H_{15}$	17.2
		$C_{28}H_{47}$	-SH	16.1
		$C_{27}H_{43}$	$-CH_5S$	14.0
		$C_{19}H_{29}S$	$-C_9H_{19}$	13.4

Parent	Oil	Fragment	Lost	Relative intensity (%)
$C_{29}H_{50}S$	Jianghan	$C_{28}H_{47}S$	$-CH_3$	100.0
		$C_{23}H_{37}S$	$-C_6H_{13}$	83.5
		$C_{22}H_{35}S$	$-C_7H_{15}$	33.4
		$C_{21}H_{33}S$	$-C_8H_{17}$	22.9
		$C_{26}H_{43}S$	$-C_3H_7$	22.5
		$C_{24}H_{39}S$	$-C_5H_{11}$	22.3
		$C_{27}H_{45}S$	$-C_2H_5$	18.2
	Rozel Point	$C_{28}H_{47}S$	$-CH_3$	100.0
		$C_{23}H_{37}S$	$-C_6H_{13}$	53.7
		$C_{22}H_{35}S$	$-C_7H_{15}$	26.6
		$C_{26}H_{43}S$	$-C_3H_7$	25.5
		$C_{28}H_{45}$	$-CH_5S$	19.2
		$C_{24}H_{39}S$	$-C_5H_{11}$	16.2
		$C_{29}H_{49}$	-SH	13.9
		$C_{27}H_{45}S$	$-C_2H_5$	13.5
		$C_{21}H_{33}S$	$-C_8H_{17}$	12.5
$C_{30}H_{52}S$	Jianghan	$C_{29}H_{49}S$	$-CH_3$	100.0
		$C_{25}H_{41}S$	$-C_5H_{11}$	26.0
		$C_{24}H_{39}S$	$-C_6H_{13}$	14.0
		$C_{28}H_{47}S$	$-C_2H_5$	11.3
		$C_{27}H_{45}S$	$-C_3H_7$	10.7
	Rozel Point	$C_{29}H_{49}S$	$-CH_3$	100.0
		$C_{29}H_{47}S$	$-CH_5$	22.3
		$C_{24}H_{39}S$	$-C_6H_{13}$	21.4
		$C_{23}H_{37}S$	$-C_7H_{15}$	21.1
		$C_{28}H_{47}S$	$-C_2H_5$	18.0
		$C_{17}H_{25}S$	$-C_{13}H_{27}$	16.2
		$C_{29}H_{47}$	$-CH_5S$	16.2
		$C_{27}H_{45}S$	$-C_3H_7$	15.7
		$C_{28}H_{47}$	$-C_2H_5S$	14.1
		$C_{25}H_{41}S$	$-C_5H_{11}$	13.4
		$C_{28}H_{43}S$	$-C_2H_9$**	12.2
		$C_{20}H_{31}S$	$-C_{10}H_{21}$	10.0

Table 3. (+) APPI CID-FTICR-MS results of class S_2• DBE 11 $C_{56\text{-}57}$ species in the Rozel Point oil. Relative intensities are normalized to the most intense daughter ion as the target peak is considered in the relative intensity calculations. Fragments with carbon or sulfur number higher than the parent peak, as well as those with relative intensity <10%, are not shown.

Parent	Fragment	Lost	Relative intensity (%)
$C_{56}H_{92}S_2$	$C_{50}H_{79}S_2$	$-C_6H_{13}$	100.0
	$C_{51}H_{81}S_2$	$-C_5H_{11}$	60.5
	$C_{55}H_{89}S_2$	$-CH_3$	14.3
	$C_{27}H_{45}$	$-C_{29}H_{47}$	13.4
	$C_{52}H_{83}S_2$	$-C_4H_9$	10.5
$C_{57}H_{94}S_2$	$C_{51}H_{81}S_2$	$-C_6H_{13}$	100.0
	$C_{52}H_{83}S_2$	$-C_5H_{11}$	100.0
	$C_{56}H_{91}S_2$	$-CH_3$	18.5
	$C_{29}H_{49}$	$-C_{28}H_{45}S_2$	16.0
	$C_{28}H_{47}$	$-C_{29}H_{47}S_2$	14.2

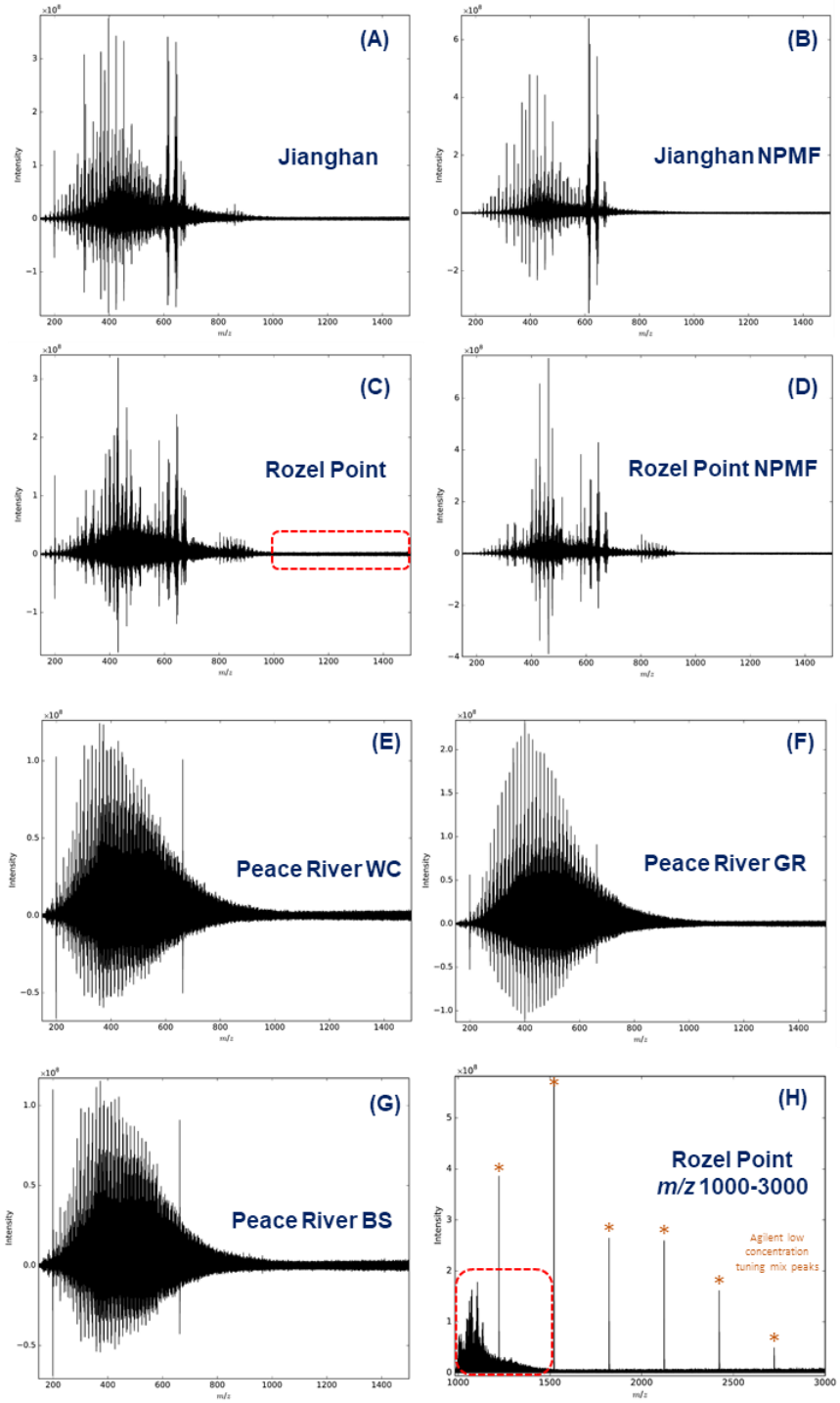

Figure 1. (+) APPI FTICR absorption-mode mass spectrum of (A-B) Jianghan oil and NPMF, (C-D) Rozel Point oil and NPMF, (E-G) Peace River oils (see Table 1 for sample codes). Plot H shows the Rozel Point oil APPI-P FTICR magnitude-mode mass spectrum, acquired from *m/z* 1000 – 3000, 100 scans, ion accumulation time increased by a 100-fold (500 ms), where the sample solution was doped with 2.5 µL of the Agilent Low Concentration Tuning Mix.

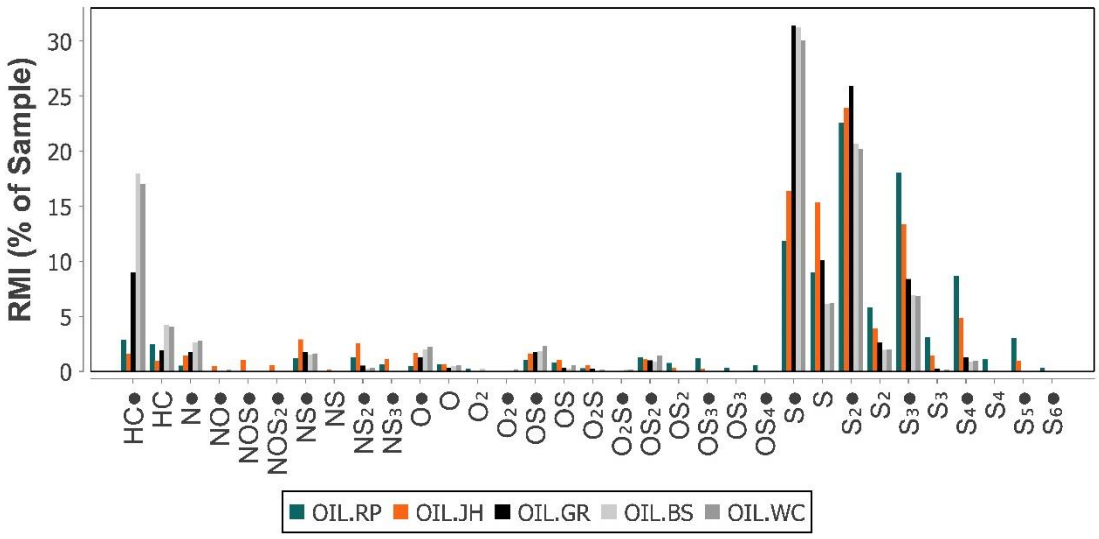

Figure 2. (+) APPI FTICR-MS compound class distribution of the oil samples analyzed in this study. Dots following class labels refer to radical ions (odd electron ion) while the absence of a dot refers to protonated ions (even electron ion). The relative monoisotopic intensity (RMI, % of Sample) is calculated as the fraction of the total monoisotopic intensities of a compound class, normalized to the sum of monoisotopic intensities of all compound classes in the sample. See Table 1 for sample abbreviations.

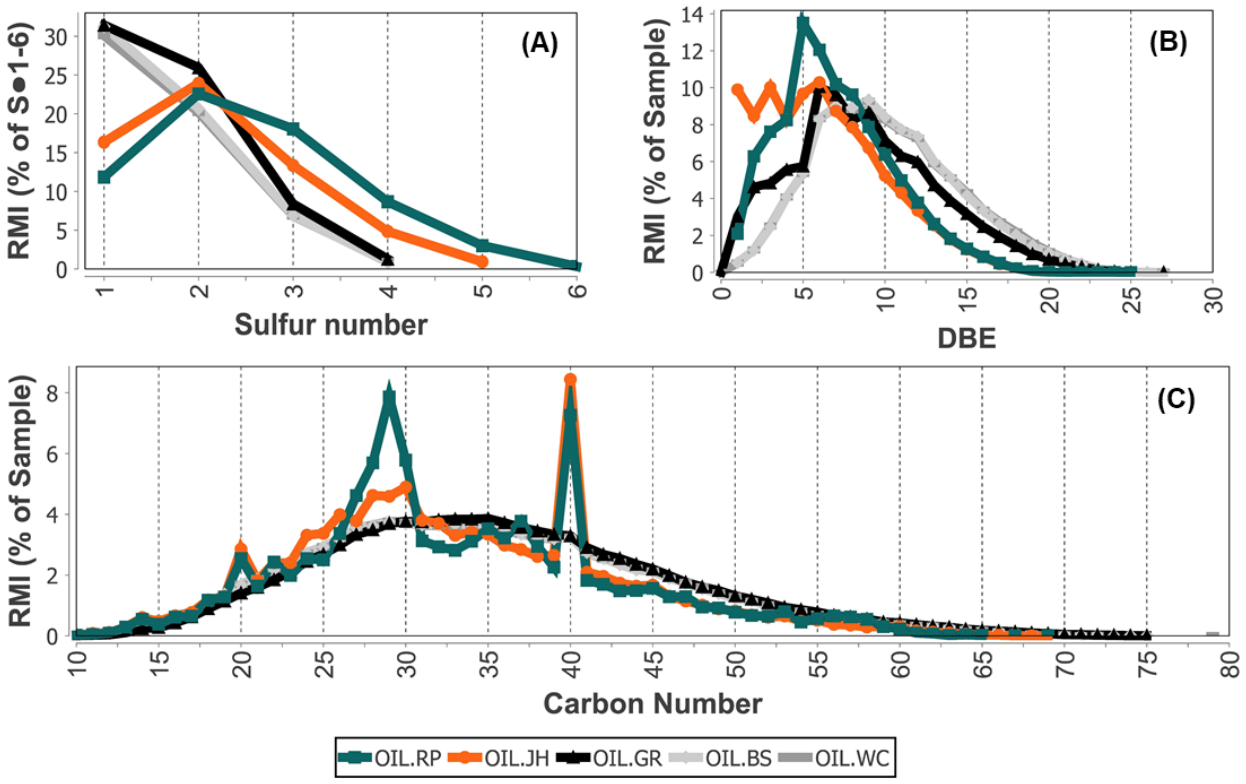

Figure 3. (+) APPI FTICR-MS parameter distributions in the oil samples analyzed in this study. (A) Sulfur number distribution, based on radical heteroatomic classes $S•_{1\text{-}6}$ peaks; (B) DBE number distribution of all assigned peaks; (C) Carbon number distribution of all assigned peaks. See Table 1 for sample abbreviations.

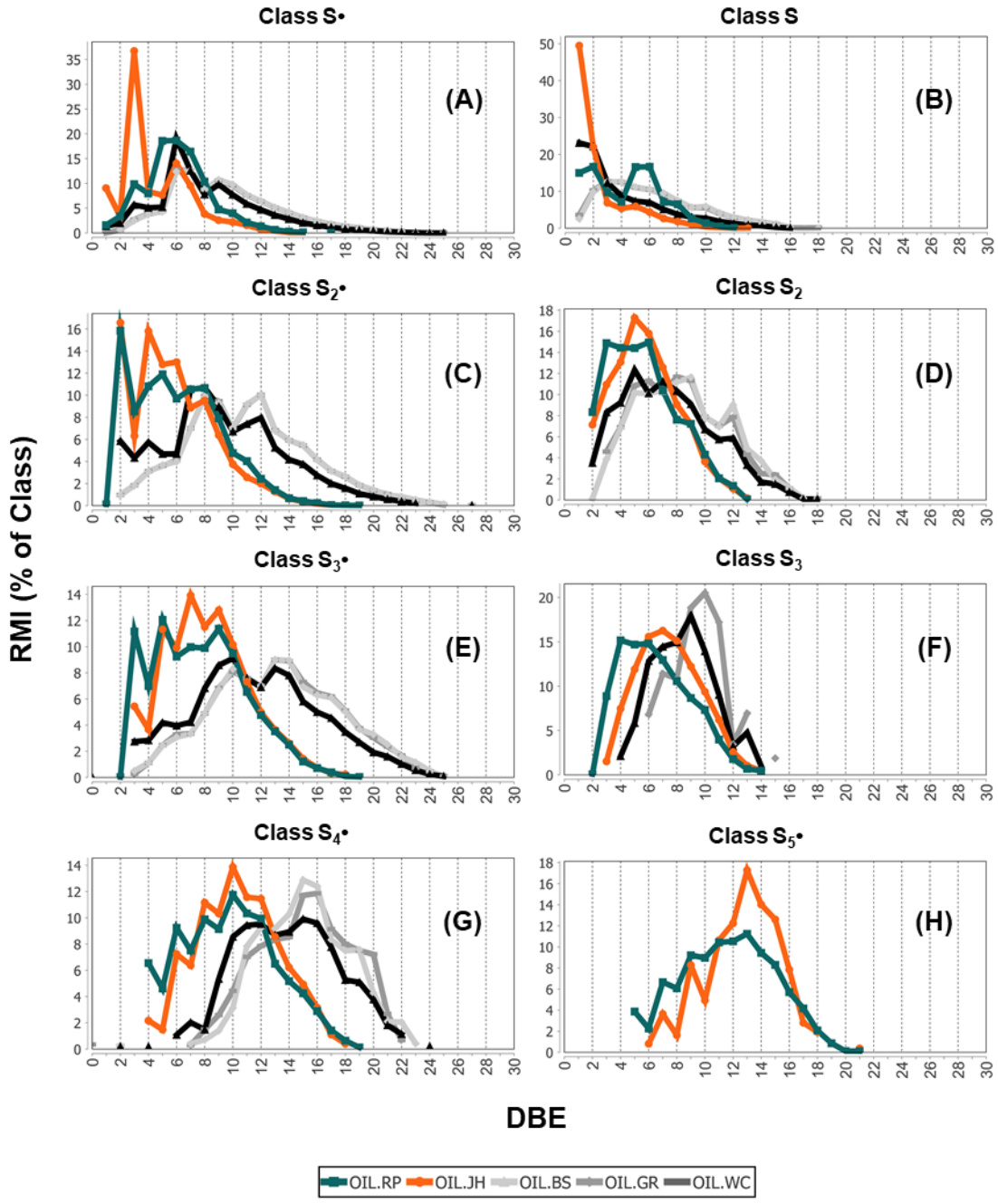

Figure 4. (+) APPI FTICR-MS heteroatomic classes S•$_{1-5}$ and S$_{1-3}$ DBE number distributions in the oil sample set. Dots following class labels refer to radical ions (odd electron ion) while the absence of a dot refers to protonated ions (even electron ion). See Table 1 for sample abbreviations.

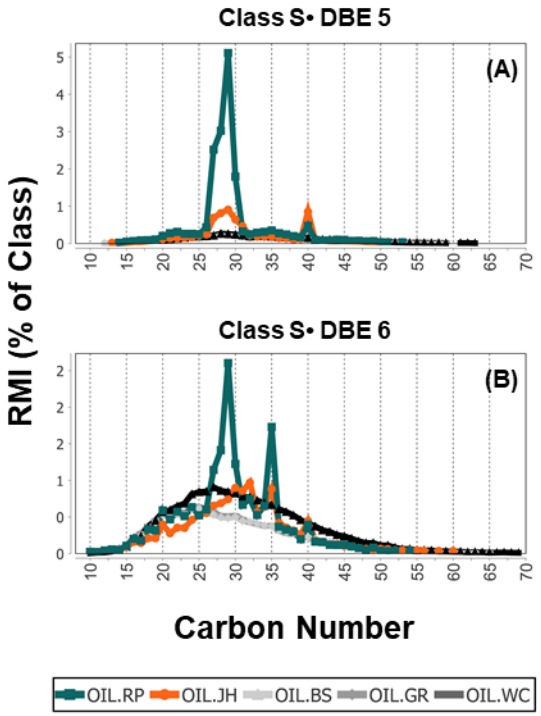

Figure 5. (+) APPI FTICR-MS carbon number distribution of heteroatomic classes $S•_1$ DBE 5 (A) and 6 (B). Dots following class labels refer to radical ions (odd electron ion. See Table 1 for sample abbreviations. Sulfurized steroid-like $C_{27\text{-}30}$ species largely dominate the class $S_1•$ DBE 5 whereas sulfurized (homo- and nor-) hopanoid-like species can be inferred from class $S_1•$ DBE 6 carbon number distribution.

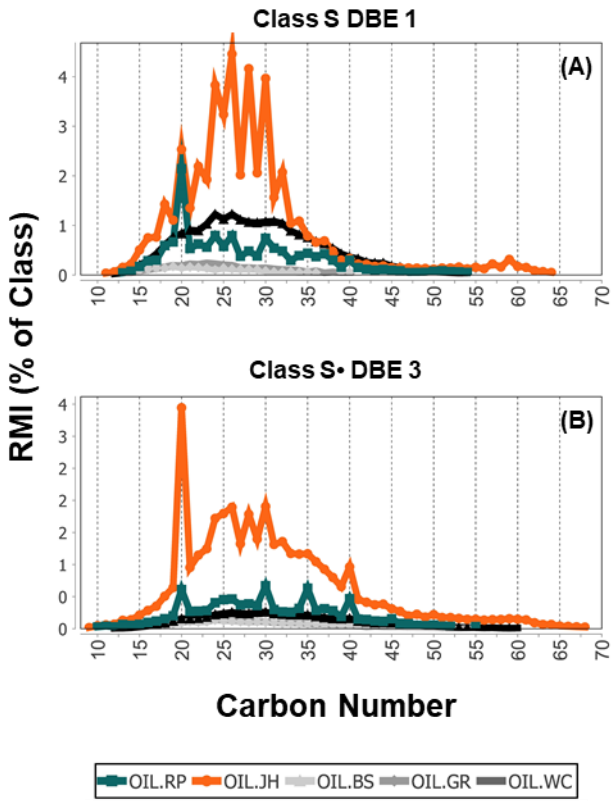

Figure 6. APPI-P FTICR-MS carbon number distribution of heteroatomic classes (A) S_1 DBE 1 and (B) S_1• DBE 3. Dots following class labels refer to radical ions (odd electron ion) while the absence of a dot refers to protonated ions (even electron ion). See Table 1 for sample abbreviations. The even/odd predominance spanning $C_{16\text{-}40}$ class S_1 DBE 1 species in Jianghan is putatively associated with alkyilthiolanes and alkylthianes. The elevated relative intensity of multiple isoprene units (x*C_5 units) in class S_1• DBE 3 species suggests an extended range of isoprenoid thiophenes in both oils but mainly in RP.

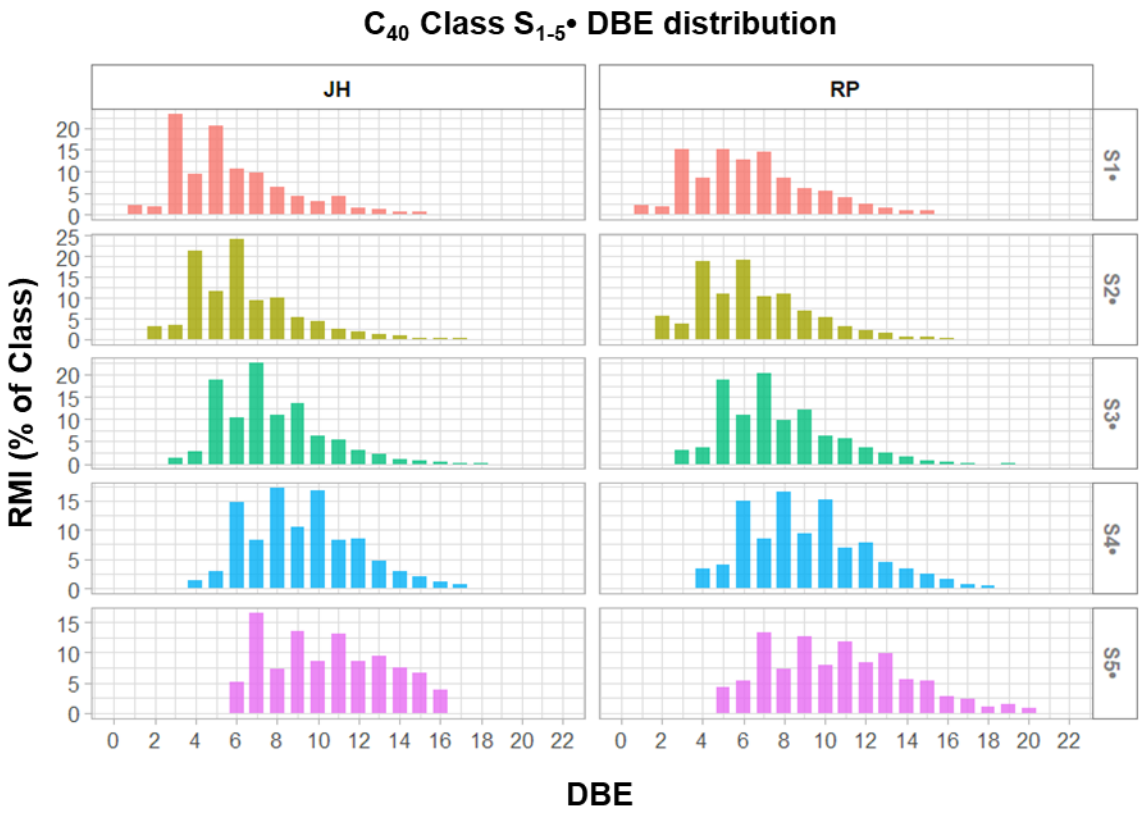

Figure 7. DBE distribution of class $S_{1\text{-}5}$• C_{40} species in Rozel Point and Jianghan oils, as detected by APPI-P FTICR-MS. An intraclass DBE = S + (2,4,6) elevated relative intensity pattern is observed and putatively associated with the number of thiophenic units in the molecules.

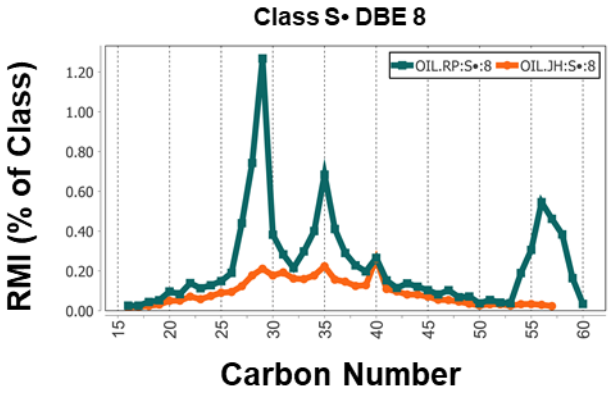

Figure 8. APPI-P FTICR-MS carbon number distribution of heteroatomic class $S•_1$ DBE 8, in Jianghan (JH) and Rozel Point (RP) oils. Dots following class labels refer to radical ions (odd electron ion). The increased elevated RMI relative intensity detected in the $C_{54\text{-}59}$ range within class $S•_1$ DBE 8 is interpreted as two $C_{27\text{-}29}$ steroidal units bridged by one sulfur atom.